Climate Dynamics (1999) 15:277–291

J. Hirschi · J. Sander · T. F. Stocker

Intermittent convection, mixed boundary conditions and the stability of the thermohaline circulation

Received: 4 November 1997 / Accepted: 5 November 1998

Abstract Intermittent convection and its consequences on the stability of the thermohaline circulation are investigated with an oceanic global circulation model (OGCM) and simple box models. A two-box model shows that intermittency is a consequence of the nonlinearity of the equation of state and of the ratio of heat and freshwater fluxes at surface versus the fluxes at depth. Moreover, it only occurs in areas, where the instability of the water column is caused by temperature or by salinity. Intermittency is not necessarily suppressed by long restoring times. Because intermittent convection causes temporal variations of the ocean-atmosphere fluxes, an OGCM cannot reach an exact equilibrium. After a switch to mixed boundary conditions, changes of the convective activity occur in areas where intermittency is observed. Intermittent convection becomes either continuous or is stopped depending on the method used for calculating the freshwater fluxes. Advective and diffusive fluxes between these regions and their surroundings change in order to balance the altered convective fluxes. A comparison between the OGCM and a six-box model illustrates that this may lead to an alteration of adjacent deep convection and of the related deep water formation.

1 Introduction

Knowledge about the stability of the thermohaline circulation is of crucial importance for the understanding of past and future evolution of the world climate. Paleoclimatic data suggest that in the past ocean circulation was different from today (e.g. Duplessy and Shackleton 1985; Sarnthein et al. 1994; Sarnthein et al. 1995). Duplessy et al. (1988) proposed that during the last glacial maximum the major deep water source was situated near Antarctica while North Atlantic Deep Water (NADW) formation was drastically reduced. Various pieces of evidence illustrate that the transition between different circulation modes has occurred abruptly during the last glacial period (e.g. Street-Perrot and Perrot 1990; Karpuz and Jansen 1992; Lehman and Keigwin 1992; Keigwin and Lehman 1994).

In modelling studies the existence of multiple equilibria of the thermohaline circulation was first observed in simple box models. Stommel (1961) showed that the thermohaline circulation may have two different regimes. More recent investigations showed that multiple equilibria of the world ocean circulation exist for highly idealized geometries (Bryan 1986; Stocker and Wright 1991; Marotzke and Willebrand 1991) and for realistic ocean basins (e.g. Hughes and Weaver 1994; Rahmstorf 1995). Transitions from one equilibrium to another were achieved with transient forcing anomalies.

Rapid transitions between different modes of the oceanic circulation comparable to that deduced from the paleoclimatic archives were simulated by Wright and Stocker (1993) and Mikolajewicz and Maier-Reimer (1994). The transition process between different equilibria was studied by Rahmstorf (1994) and Lenderink and Haarsma (1994). They showed that ocean models respond to slowly varying atmospheric forcing by sudden changes of the convection pattern, which lead to a change of the thermohaline circulation.

Rapid changes of the ocean circulation are also observed after the transition from restoring boundary conditions to more realistic ocean–atmosphere fluxes. Bryan (1986) observed a spontaneous interruption of the thermohaline circulation (halocline catastrophe) if the ocean-atmosphere fluxes were switched to mixed boundary conditions. Marotzke (1991) showed that this can be prevented if the standard convection scheme of Bryan (1969) is replaced by an algorithm that guarantees a complete removal of static instabilities or by an implicit vertical mixing. However, even if

J. Hirschi (✉) · J. Sander · T. F. Stocker
Climate and Environmental Physics, Physics Institute,
University of Bern, Sidlerstr. 5, CH-3012 Bern
E-mail: jocl@climate.unibe.ch

the convection scheme of Marotzke (1991) is applied, the ocean circulation shows substantial changes after the transition to mixed boundary conditions (Marotzke and Willebrand 1991). A study by Tziperman et al. (1994) suggests that the stability by the thermohaline circulation can be increased when long restoring times are used for sea surface salinity. In a recent work Cai (1996) showed that the assumption of a zero-heat capacity atmosphere, in which the surface air temperature is balanced between the sea surface temperature and a radiative equilibrium temperature stabilizes the thermohaline circulation.

The aim of this study is to investigate the mechanisms responsible for the sensitivity of the deep circulation to changes of the boundary conditions. We will show that these mechanisms are related to intermittent convection in an OGCM. For this purpose we investigate the convective processes with the help of very simplified box models. This approach is similar to that of Pierce et al. (1995) who analyzed oscillations of the convective activity in the Southern Ocean.

However, Pierce et al. (1995) focused on centennial oscillations which occurred under mixed boundary conditions. Intermittent convection observed in our study occurs under restoring boundary conditions and has periods of a few months. In contrast to the study of Pierce et al. (1995), where convection is switching on and off in the whole area of southern deep water formation, intermittent convection observed in our study is limited to the surface layers of a few grid cells. The time needed for destabilizing the water column after a convective event is given by the restoring time and the horizontal advective and diffusive fluxes between adjacent grid cells. In our numerical experiments these times are typically on the order of a few months which corresponds to the length of the convective periods.

The outline of this study is as follows. After a brief description of the numerical model we analyze the convective processes in an OGCM under restoring boundary conditions with a simple 2-box model. Then, different evolutions of the ocean circulation obtained after transition to mixed boundary are presented. Finally, a spontaneous breakdown of deep water formation simulated in the Southern Hemisphere is investigated in detail using a six-box model.

2 Model description

We use the well-known Bryan–Cox ocean general circulation model of Bryan (1969) in the version of Pacanowski (1995). The global ocean is represented by two basins of equal angular width of 60° each extending from 75 °S to 75 °N in latitude. A freely evolving Antarctic Circumpolar Current (ACC) connects the two basins in the south between 50 °S and 65 °S. The southernmost parts of the basins between 65 °S and 75 °S are marginal basins, representing an idealized Ross and Weddell Sea. Very similar geometries have been used by Marotzke and Willebrand (1991) and Rahmstorf and Willebrand (1995).

The bottom at 5000 m depth is flat. The only exception is at the connection of both basins between 5 °W–5 °E and 50 °S– 65 °S where a 2500 m deep sill builds a partial barrier. The horizontal resolution is 2.5° in latitude and longitude while the vertical is divided into 19 levels of varying thickness ranging from 30 m at the surface to nearly 550 m in the bottom layer.

Until a steady circulation is reached, temperature and salinity are restored to zonally uniform profiles based on analytical functions. The temperature follows roughly a zonal mean of observed surface values in the Atlantic (Levitus et al. 1994). Wind stress also depends only on latitude (Fig. 1).

Restoring salinity roughly follows the zonal mean between 30 °W and the Greenwich Meridian (GM) (Levitus and Boyer 1994). This explains the salinity plateau at 50 °N which reflects the transport of salty water to high northern latitudes. By the use of a zonal mean of the whole Atlantic basin, surface salinity would be too low in the northern deep water formation areas to allow a reasonable rate of deep water formation. The sharp increase of salinity between 60 °S and 75 °S is motivated by the fact that the salinity values observed around Antarctica at a depth of a few hundred metres are about 34.7, which corresponds to the salinity of Antarctic Bottom Water (AABW) (Levitus and Boyer 1994). A similar approach has already been used in other studies e.g. England (1993).

Horizontal viscosity and diffusivity coefficients are set to $2.5 \cdot 10^5\,m^2s^{-1}$ and $2.5 \cdot 10^3\,m^2s^{-1}$, respectively, the vertical coefficients are $10^{-4}m^2s^{-1}$. Instabilities of the water column are removed by using the convection scheme of Marotzke (1991) which guarantees complete removal of static instabilities.

For the spinup, restoring times of 30 days and 150 days are used. Integration is carried out for 7000 y until the variations of deep sea temperature are less than 0.01°C/1000 y. The experiments with restoring times of 30 days and 150 days are denoted by R30 and R150, respectively.

The horizontal and global meridional mass transports for experiment R30 are shown in Fig. 2. The barotropic transport shows the typical sub-polar, mid-latitude and tropical gyres in both basins. With a mass transport of about 44 Sv, the ACC is too weak compared to observational estimates of about 125 Sv (Whitworth and Peterson 1985). Meridional overturning cells occur at high northern and southern latitudes in both basins. In contrast to Weaver and Sarachick (1990) the deep cell observed at the equator may not be due to numerical instability. As in Klinger and Marotzke (1997) it remained present when the vertical resolution or the vertical

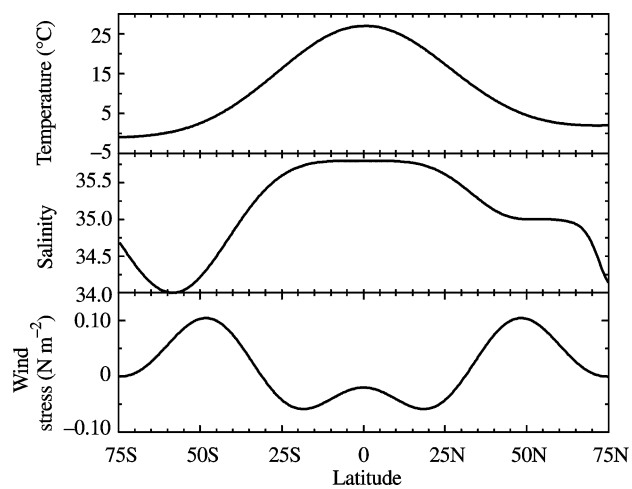

Fig. 1 Forcing profiles for temperature, salinity and wind stress. Temperature and salinity are based on analytical functions following zonal averages of surface values in the Atlantic, while wind stress is based on a zonal average of the surface values over the global ocean

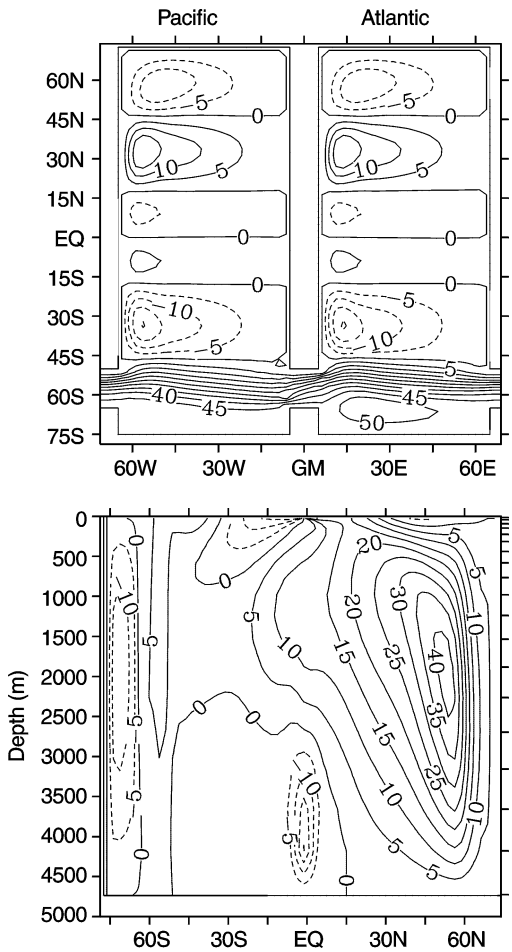

Fig. 2 Geometry and horizontal mass transport (*upper panel*) and global meridional overturning (*lower panel*) after 7000 y for experiment R30. Units for mass transport are Sv ($1\,\mathrm{Sv} = 10^6\,\mathrm{m}^3/\mathrm{s}$)

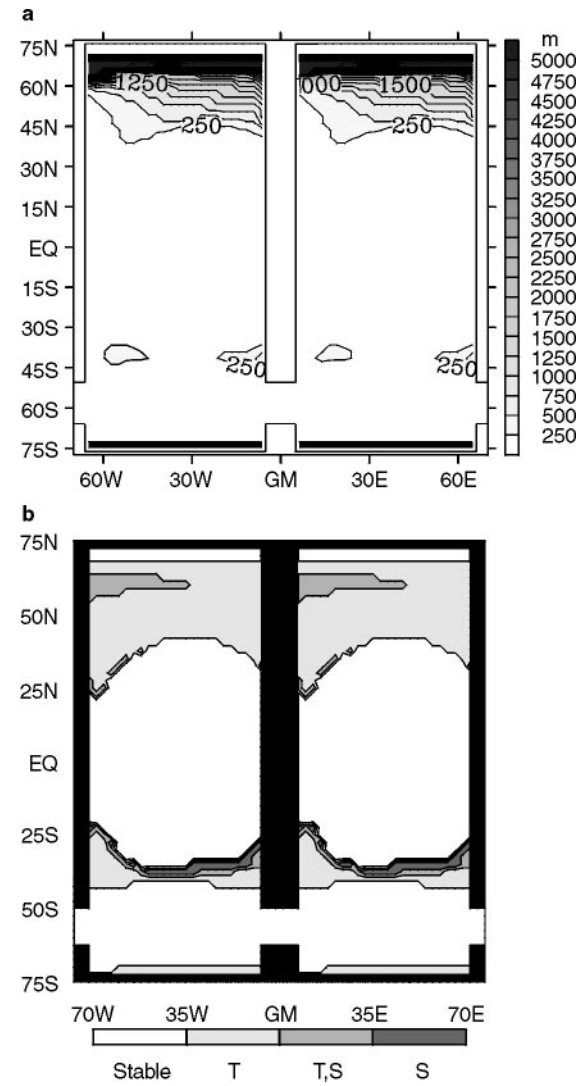

Fig. 3 a Convection depth in m for experiment R30. **b** Geographical location of different types of convection. Temperature driven adjustment is denoted by T, salinity driven adjustment, S and the mixed type of temperature and salinity instability, T,S. Data represent mean values over 5 y

diffusivity were increased. Single basin experiments of Klinger and Marotzke (1999) show that the equatorial overturning cell occurs in case of "slightly asymmetric" circulation i.e. when deep water is formed at different rates in the northern and southern parts of the basin. No deep equatorial cell is observed if deep water formation occurs only in the northern or in the southern part of the basin.

3 Different types of intermittent surface convection

In the real world deep water is formed in the northern and southern high latitudes due to different mechanisms. According to Killworth (1983) the analysis of water masses shows that near–surface waters with an enriched salinity and warm temperature are transported into the northern area, where strong cooling leads to deep convection. Around Antarctica, on the other hand, the surface waters are near the freezing point, and during ice formation the release of brine leads to deep water formation (Carmack 1986). Both mechanisms result in an unstable water column and rapid vertical mixing.

Figure 3a shows the areas where deep convection occurs in the OGCM for experiment R30. In the Northern Hemisphere convective adjustment sets in at about 45 °N with near–surface mixing and reaches the bottom between 65 °N and 70 °N. This can be explained by a salinity plateau between 45 °N and 65 °N, where salinities are almost constant while temperature decreases towards the north, so that surface densities increase with latitude (Fig. 1). In the south, deep convection is restricted to the southernmost line of grid cells. Marginal stability characterizes the Weddell and Ross Sea for experiment R30 while in experiment R150 convection sets in at the southern border of the Antarctic Circumpolar Current (ACC). In both experiments instability of the water column also occurs at the northern border of the ACC.

Note that convective adjustment gives rise to meridional overturning of the water masses but must be clearly distinguished from it. At zonal boundaries convection can trigger east–west pressure gradients, which drive meridional overturning. In our model geometry this leads to the northern and southern overturning cells depicted in Fig. 2.

With the convective adjustment scheme both the temperature and salinity of a grid box are instantaneously mixed with those of the underlying box. In the upper box the temperature can increase or decrease depending on whether the water column was stable with respect to temperature or not. Because the same holds true for salinity, three different cases of an unstable water column are possible, see Table 1. If the water column is stable with respect to salinity ($\partial S/\partial z \leq 0$), convective adjustment will lead to increased temperature and salinity of the upper grid box. Conversely, if the column was thermally stable ($\partial T/\partial z \geq 0$), the mixing reduces temperature and salinities of the upper layer. In the case of instability of both variables, convective adjustment will increase temperature and decrease salinity of the upper box. Therefore, the different types of mixing result in different changes of the atmosphere-ocean heat and salt fluxes. Note that the instability of the water column due to temperature *and* salinity can only occur between two successive passes of the adjustment scheme. In that case, advective, diffusive and restoring fluxes of heat and salt have a permanent destabilizing effect. This state can only remain as long the water column is not checked for stability. In the other two cases the instability can remain for a long time.

We have calculated temperature and salinity of the surface to classify which type results in convective mixing of the surface layer in the OGCM for experiment R30. In Fig. 3b the global ocean is divided into different areas depending on the kind of instability which leads to convection at the surface. The areas were obtained by comparing the surface values of temperature and salinity before and after the application of the convection scheme. Unchanged temperatures and salinities indicate that no instability occurred. Depending on an increase or decrease of temperature and salinity the type of the convective mixing was identified.

In most convective active areas a negative temperature gradient contributes to the instability of the surface layer, i.e. the surface is thermally unstable. This follows climatological data (e.g. Levitus et al. 1994; Levitus and Boyer 1994). Moreover, the temperature-driven instability is found in the Southern Hemisphere, where deep water forms and the whole water column is mixed. In the Northern Hemisphere, instabilities due to salinity are found only in connection with an instability due to temperature in the western parts of both basins at about 60 °N. This can be explained by the fact, that temperature–driven deep convection between 65 °N and 70 °N brings salt to the surface. It is transported southward by the western boundary currents of the sub-polar gyres (Fig. 2), and increases the contribution of salt to instability.

Table 1 Stratification of two underlying grid boxes leading to convective adjustment, z is positive upward

	T driven	S driven	T and S driven
Temperature	$\partial T/\partial z < 0$	$\partial T/\partial z \geq 0$	$\partial T/\partial z < 0$
Salinity	$\partial S/\partial z \leq 0$	$\partial S/\partial z > 0$	$\partial S/\partial z > 0$

At the northern boundary of the circumpolar current all three types of instability are observed. In this area cold, less saline circumpolar water mixes with warmer, saltier mid-latitude water. Water masses adjacent to the circumpolar current are dominated by low temperatures and low salinities, so instabilities are caused by temperature there. In the latitudinal band between 40 °S and 20 °S the destabilizing influence of temperature decreases, while it increases for salinity. In a narrow belt between 40 °S and 20 °S instability is caused by both temperature and salinity or by salinity only. Further north, high temperatures stabilize the water column. This follows closely the profiles of the restoring temperature and salinity (Fig. 1).

In order to determine the areas, where intermittent convection occurs in the OGCM, we examined the maximum and minimum surface freshwater flux during five years at the end of the spinup. The differences between the maximum and minimum values are plotted in Fig. 4a. The strongest variations occur in the Southern Hemisphere where convection is temperature driven. There, amplitudes of the variations reach more than 0.6 m/year. In the rest of the basins these variations are at least two orders of magnitude smaller. Figure 4b shows time series over five years of the restoring fluxes of salt and heat, for a single grid box with strong variation of the freshwater flux at (37.5 °S/57.5 °W). Convective events are visible as abrupt changes of the freshwater and heat fluxes. Each convective event causes a sudden decrease of the freshwater flux of about 25 cm/y and about 6 Wm^{-2} for the heat flux. This rise and breakdown of convection introduces intermittency which indicates that the ocean reaches a steady state only in a statistical sense.

3.1 Convection in a simple two-box model

Here we use a two-box model as a simple tool to study all three cases of instability. This model is similar to the flip–flop mechanism presented by Pierce et al. (1995) or Lenderink and Haarsma (1994) (Fig. 5). The boxes represent the two uppermost ocean layers. The values H_1 and Y correspond to the thickness of the surface layer and to the meridional extent of a grid cell of the three-dimensional model, respectively. The equations

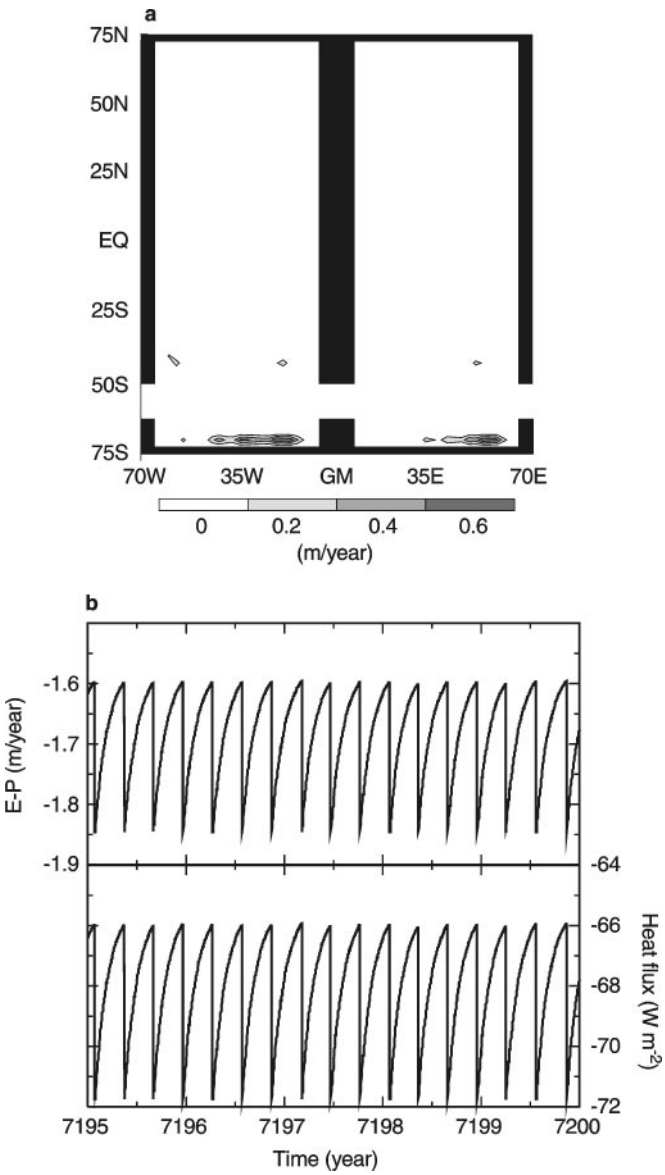

Fig. 4 **a** Variation of the freshwater flux under restoring boundary conditions. **b** Time series of freshwater flux and heat flux from the ocean to the atmosphere for a typical grid cell at 37.5 °S/57.5 °W with intermittent convection. Adjacent grid cells are not convecting intermittently

for temperature and salinity read:

$$\frac{dT_1}{dt} = \gamma(T^* - T_1), \tag{1}$$

$$\frac{dT_2}{dt} = U\frac{|\Delta\rho|}{\rho_0}\frac{(T_3 - T_2)}{Y} + K_d\frac{(T_3 - T_2)}{Y^2}, \tag{2}$$

$$\frac{dS_1}{dt} = \gamma(S^* - S_1), \tag{3}$$

$$\frac{dS_2}{dt} = U\frac{|\Delta\rho|}{\rho_0}\frac{(S_3 - S_2)}{Y} + K_d\frac{(S_3 - S_2)}{Y^2}, \tag{4}$$

$$|\Delta\rho| = |\rho_3 - \rho_2|. \tag{5}$$

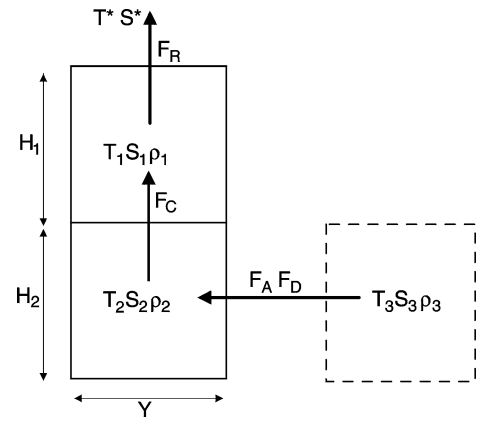

Fig. 5 Two-box model for analyses of convection. The boxes have thicknesses H_i and length Y with temperature T_i, salinity S_i and density ρ_i. T^*, salinity S^* are the restoring values for temperature and salinity at the surface. T_3, S_3 are kept constant so that the dashed box is like an infinite reservoir of heat and salt. Exchange of heat or salt is obtained by advective, diffusive, restoring and convective fluxes F_A, F_D, F_R and F_C. Parameter values are given in Table 2

Table 2 Model parameters for the two-box model

Parameter	Definition	Value
H_1	Surface box thickness	30 m
H_2	Lower box thickness	30 m
Y	Meridional extent	$2.77 \cdot 10^5$ m
K_d	Diffusivity	$2.5 \cdot 10^3$ m^2/s
U	Advective velocity	40.5 m/s
ρ_0	Reference density	1000 kg/m^{-3}
$1/\gamma$	Restoring time	30 days

Advection and diffusion coefficients are denoted by U, K_d and the inverse restoring time scale by γ. K_d and γ are chosen according to the three-dimensional model. Advection is proportional to the horizontal density difference with advective velocity in the order of $(U\Delta\rho)/\rho_0 \approx 10^{-3}$ m/s.

All parameters are shown in Table 2. If convection occurs ($\rho_1 > \rho_2$), temperature and salinity are homogenized with a volume-weighted average according to

$$T = \frac{H_1T_1 + H_2T_2}{H_1 + H_2}, \quad S = \frac{H_1S_1 + H_2S_2}{H_1 + H_2}.$$

For the densities the full equation of state of sea water (UNESCO 1981) is used. The densities are calculated for the pressure at depth H_1. The model equations are solved with the explicit Euler forward scheme.

The arrangement of the two-box model allows us to reproduce convection induced by temperature, salinity or by both and to examine whether intermittency occurs. In order to obtain intermittent temperature or

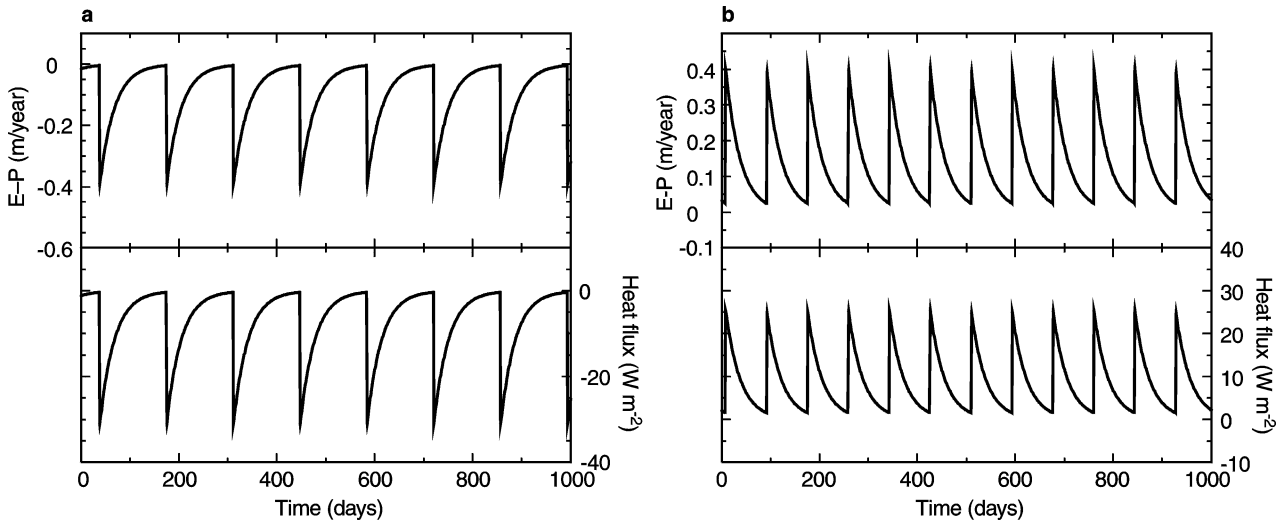

Fig. 6a,b Restoring fluxes of heat in Wm^{-2} and salinity in m/y, for intermittent convection simulated in the two-box model. **a** Temperature driven convection, **b** salinity driven convection

salinity driven convection, the restoring values T^*, S^* and the reservoir temperature and salinity T_3, S_3 were chosen so that their densities are nearly identical. Instability was obtained by small changes of the restoring values (this is also possible by changing S_3 or T_3). Figure 6 shows time series of the restoring fluxes for temperature and salinity.

Temperature-driven convection is shown in Fig. 6a and salinity driven convection in Fig. 6b. The mixed type of temperature and salinity driven convection is always continuous and not intermittent. Note that the temperature evolution of temperature–driven convection (Fig. 6a compares well with that of the OGCM, see Fig. 4b).

The reasons for intermittency are clarified in a schematic T–S diagram shown in Fig. 7. Consider two water masses one above the other. The water at the surface is forced towards S^* and T^* by restoring, while temperature and salinity of the lower water are determined by advection and diffusion. Figure 7 shows different conditions under which convection can occur. Surface waters are indicated by 1 or 3 in Fig. 7, lower water is denoted by 2. First we consider water masses 1 and 2 which occupy the same isopycnal and are neutrally stable with respect to each other. Convection is induced when water mass 1 cools or becomes saltier. The instability is then caused by temperature, because salinity in the upper box remains smaller than that of the lower box, see also Table 1. The density of the mixture of both water masses is larger than the initial one. After convection salinity and temperature are driven towards their initial values 1 and 2 by restoring or advection and diffusion, respectively. The surface water and the lower water become less dense. If restoring fluxes are stronger than advection and diffusion at depth, surface water becomes less dense than the lower water, which stabilizes the water column. Convection is

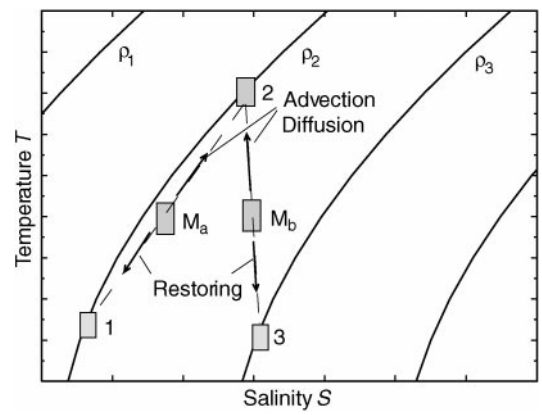

Fig. 7 Illustration of the different types of convection in a schematic T–S diagram. For temperature-driven convection, water masses 1 and 3 represent surface waters, while 2 is the water mass below. Salinity driven convection is obtained with an interchange of water 1 and 2. The mixture of waters 1 and 2 is denoted M_a. For temperature *and* salinity driven convection mixture M_b is obtained from water masses 2 and 3

re-initiated when salinities and temperatures are again on a common isopycnal. For our box model this is always the initial isopycnal, i.e. convection restarts when the temperature and salinity have reached their initial values. Between successive convective events, the water column is stable. In this case convection is intermittent.

If the water masses 1 and 2 are interchanged (an instability is then induced with a denser water mass 2), we can induce a salinity driven convection. Here again, stable phases can occur between convective events if restoring is stronger than advection and diffusion.

An example for temperature and salinity driven convection is shown in Fig. 7 with the water masses 2 and 3. The two water masses are already unstable.

Their mixture is more dense than water mass 2 but less dense than 3. Restoring fluxes make the surface water denser, while advection and diffusion lighten the water at depth. Stable phases as observed in the temperature or salinity driven cases are not possible here, convection can only be continuous.

A prerequisite for intermittency is the non-linearity of the equation of state, that allows a mixture which is denser than surface water just before convection. Using a linear equation-of-state suppresses intermittency. In the heat-salt oscillator of Welander (1982) intermittent convection was obtained with a linear equation-of-state, because different restoring times were used for temperature and salinity.

Intermittency occurs when the mixed water reaches the initial density of the surface water earlier than that of the deep water (Fig. 8 a). The mixed water mass M is found on the mixing line at a position depending on the volumes of the water masses. The time for mixed water to reach its original value corresponds to the time to pass from M to 2 and from M to 1. For the two-box model these times are determined by the advective/diffusive time scales and the restoring time, respectively. Therefore, intermittency is determined by three parameters: the ratio of the volumes or depths H_2/H_1, the advection/diffusion time scales and the restoring time. For small ratios of H_2/H_1 the lower water will eventually pass through denser waters to reach its initial value (Fig. 8b). This prolongs the periods between convective events. Increasing the restoring time will decrease the amplitude of the ocean-atmosphere fluxes (Fig. 9a). Eventually intermittency ceases and convection becomes continuous. However, long restoring times do not necessarily suppress intermittency. As shown in Fig. 9b the intermittent convection will reappear if advection and diffusion are reduced. The frequency of convective events therefore decreases with increasing ratio of the restoring flux versus the advective and diffusive fluxes at depth.

Similar features can be observed in the OGCM. Figure 10 shows the densities at location 37.5 °S/57.5 °W for experiment R30. The typical situation of intermittent convection is represented. One layer with depth H_2 found between a permanently mixed upper water column of total depth H_1 and the stable stratified deep water is frequently involved in the convective process. Because $H_2/H_1 < 1$ the evolution of the respective densities follows closely the findings of the two-box model (Fig. 8b, lower panel).

For experiment R150 intermittency occurs in areas adjacent to the southern and northern borders of the ACC. The maximum amplitudes of freshwater fluxes are about 3 cm/y. Increasing the restoring time reduces the amplitudes of temporal variations of the freshwater flux by more than a factor of 10 but do not suppress them.

4 Transition to mixed boundary conditions

4.1 Experiments

A steady state circulation is a prerequisite for a smooth transition to mixed boundary conditions because only then are the fixed freshwater fluxes used under mixed

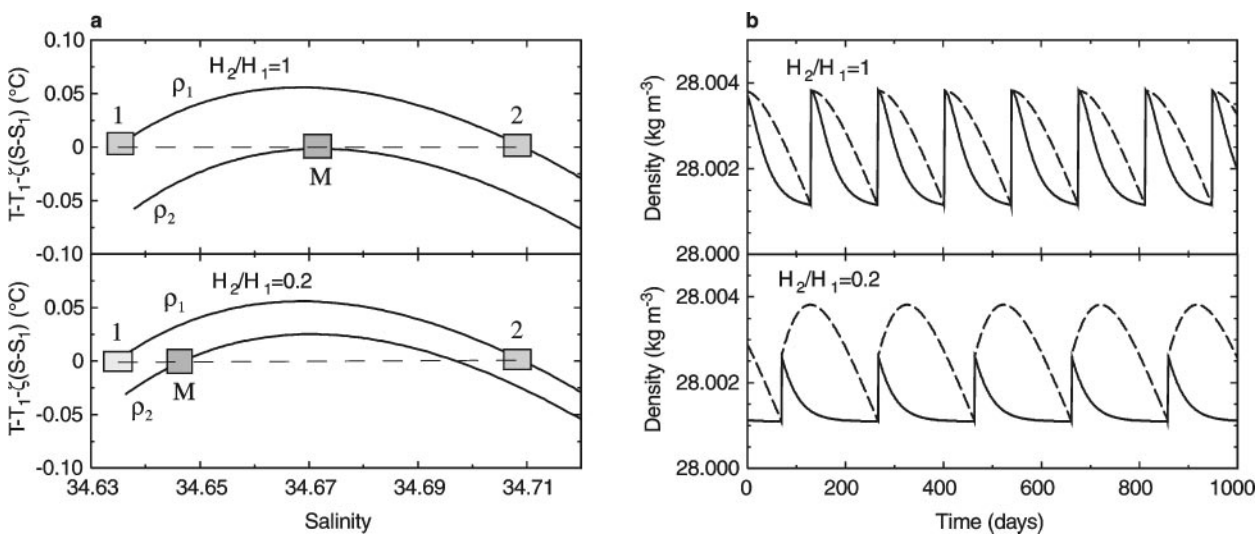

Fig. 8 a Modified T–S diagrams for the two-box model. For convenience a straight line $T = T_1 + a(S - S_1)$ with $a = (T_2 - T_1)/(S_2 - S_1)$ is subtracted from the temperature values of ρ_1 and ρ_2. Parameters chosen: $H_2/H_1 = 1$ and 0.2, $T_1 = -1.0\,^{\circ}\mathrm{C}$, $T_2 = 0.51\,^{\circ}\mathrm{C}$, $S_1 = 34.635$ and $S_2 = 34.735$. Surface water is denoted by 1, deep water by 2 and the mixture by M. The isopycnals are denoted by ρ_1 and ρ_2 ($\rho_1 < \rho_2$). **b** Time evolution of densities at surface (*solid lines*) and depth (*dashed lines*) for intermittent convection in the two-box model

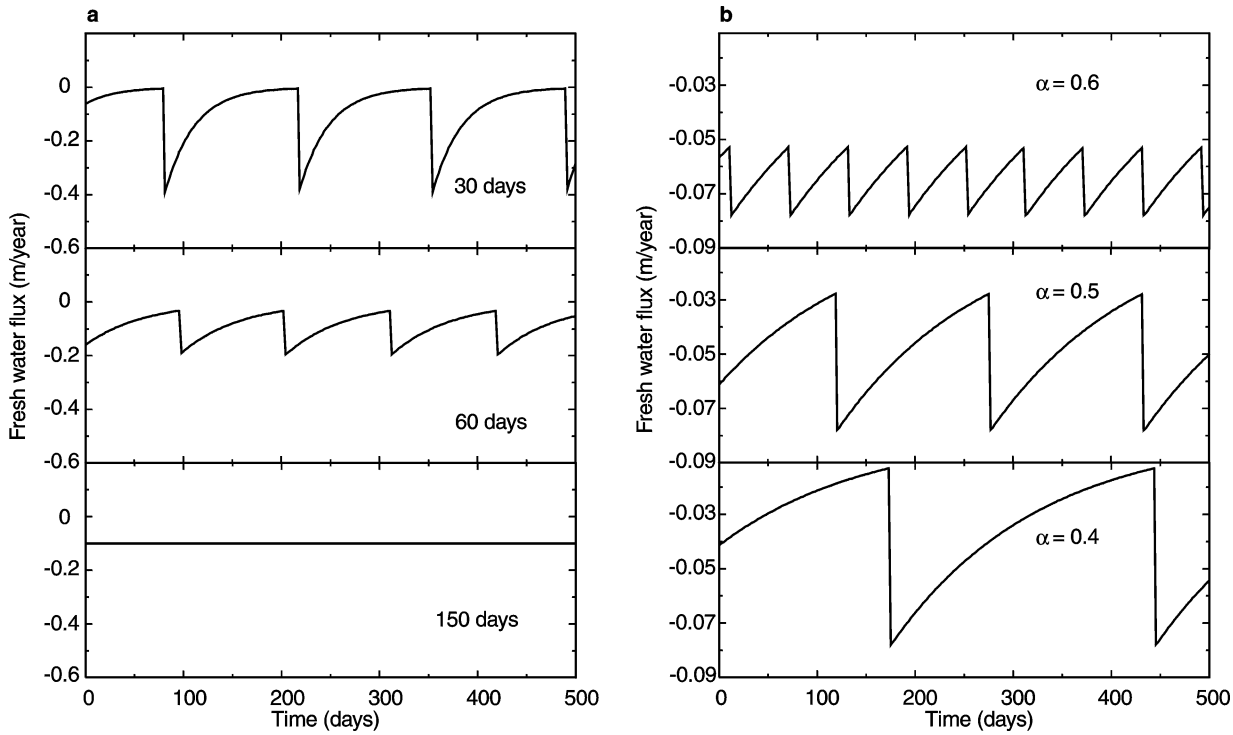

Fig. 9a,b Restoring freshwater flux for different restoring times or advection rates in case of intermittent convection with $H_2/H_1 = 1$. **a** Restoring times are 30 days, 60 days and 150 days, respectively. **b** For a restoring time of 150 days the advection and diffusion coefficients U and K_d are both changed by a factor α of 0.6, 0.5 and 0.4

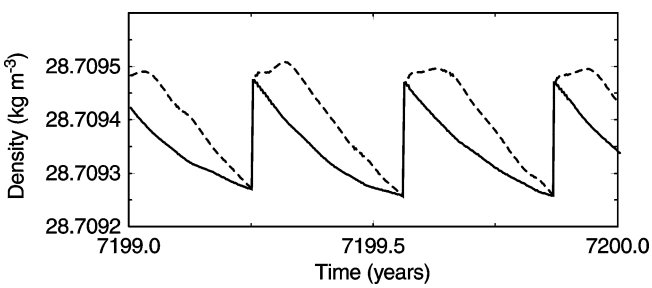

Fig. 10 Intermittent convection in 37.5 °S/57.5 °W in the OGCM. The *solid line* shows the density $-1000\,\mathrm{kg\,m^{-3}}$ of the homogenized layers 1–5 with total thickness $H_1 = 270$ m, the *dashed line* the density $-1000\,\mathrm{kg\,m^{-3}}$ of layer 6 with $H_2 = 107$ m

Table 3 Experiments under mixed boundary conditions (MBC)

Experiment	Restoring time for spinup	Switch to MBC
30A	30 days	Instantaneous
30B	”	Time mean over 100 years
30C	”	Lowest values of SSS
30D	”	Highest values of SSS
150A	150 days	Instantaneous
150B	”	Time mean over 100 years
150C	”	Lowest values of SSS
150D	”	Highest values of SSS

boundary conditions and the restoring fluxes identical. Even after a spinup of several thousands of years, however, restoring fluxes are not necessarily constant because of intermittent convection. Therefore, the circulation achieved with restoring fluxes during spinup may change once a fixed freshwater flux is prescribed under mixed boundary conditions. This was first observed by Bryan (1986).

The initial states for the experiments under mixed boundary conditions are given by circulations achieved in experiments R30 and R150. Four different types of sea surface salinity fields are employed for calculating the freshwater flux E–P (*evaporation* — *precipitation*): (A) instantaneous salinity field at the time of switch to mixed boundary conditions; (B) time mean over the last 100 y before the switch; (C) lowest or (D) highest salinity, which occurred in each grid cell, during the last 5 y of the spinup. An overview of the experiments under mixed boundary condition is given in Table 3. The

Fig. 12a,b Meridional overturning after transition to mixed boundary conditions (at *time* = 7200 y) for the experiments starting from experiment R30. **a** experiments with different evolutions of the Pacific and Atlantic circulations. **b** similar evolution in both basins. Refer to the text for details

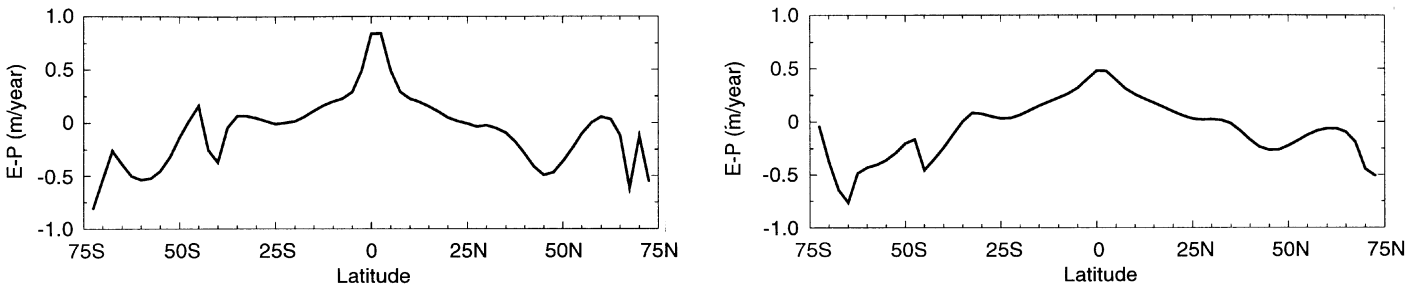

Fig. 11 Zonal mean of freshwater flux for the initial states achieved under restoring times of 30 days (*left panel*) and 150 days (*right panel*)

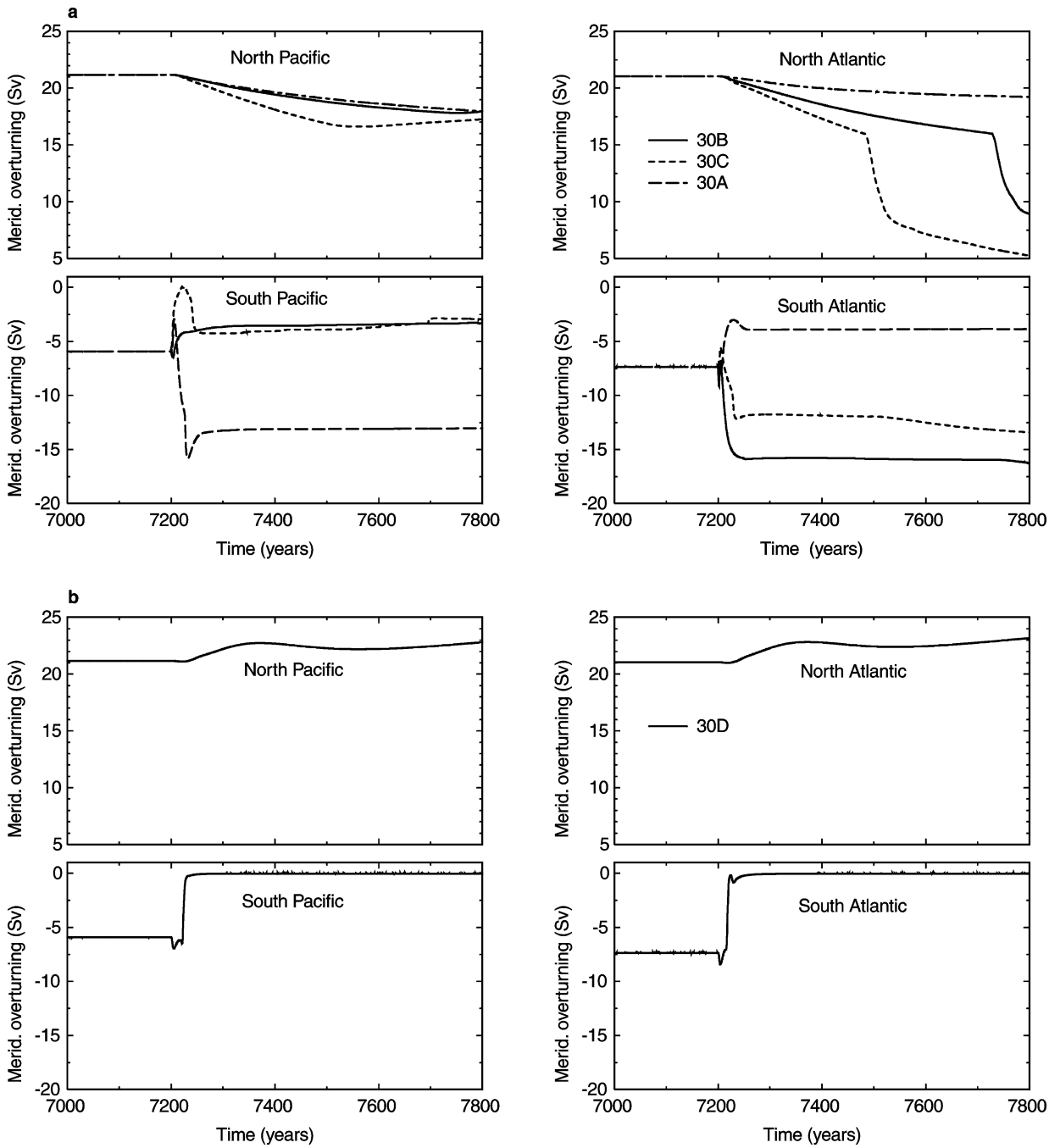

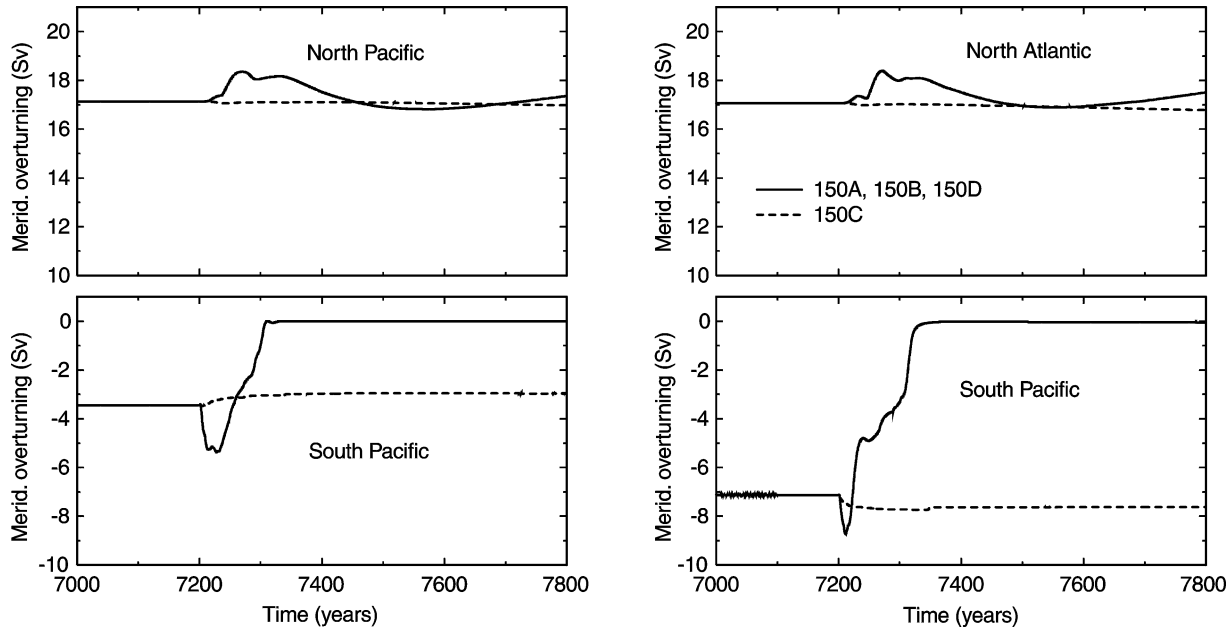

Fig. 13 Evolution of the northern and southern deep water overturning cells. Experiments starting form the 150 days spinup all lead to similar evolutions of the circulation in both basins

freshwater flux is calculated according to

$$E - P = \frac{\gamma \cdot D}{S_0}(S^* - S), \tag{6}$$

where D is the thickness of the uppermost ocean layer, S_0 a reference salinity of 35, γ the inverse restoring time and S^* the restoring salinity. The value of S is determined according to one of the four methods just described. Note that the global mean of E–P is subtracted in order to guarantee the conservation of salt. The zonal means of freshwater fluxes calculated at the end of experiments R30 and R150 are shown in Fig. 11.

The transient behaviour after switching to mixed boundary conditions is depicted in Fig. 12 for experiments starting from R30 and in Fig. 13 for experiments starting from R150. Both figures show the evolution of the maximum meridional overturning north of 30 °N and south of 30 °S below a depth of 500 m. Except for experiment 150C (Fig. 13), where the circulation shows only small alterations, important changes occur in the overturning cells. In these cases the southern overturning cells show strong increases or decreases during the first decades under mixed boundary conditions. In the Northern Hemisphere changes evolve less rapidly during the first decades under mixed boundary conditions. However, drifts are still present in the northern cells even though no significant further changes of the southern cells can be observed (years 7250–7500). Abrupt decreases of the North Atlantic cell occur after 300 y in experiment 30C and after about 530 y in experiment 30B. This development is probably related to the increased meridional overturning in the South Atlantic and is not fully understood yet.

5 Intermittent convection and southern ocean circulation

This section illustrates how intermittency leads to the collapse of deep water formation in the Southern Hemisphere seen in experiment 30D. A comparison of the freshwater flux and surface heat flux obtained from the OGCM and the two-box model is given in Fig. 14. The aperiodicity of the OGCM fluxes is due to an interaction with other sites of intermittent convection. According to experiment 30D, the freshwater flux for the two-box model was calculated with the highest salinity value, which occurred during the last five years under restoring boundary conditions. The resulting most negative freshwater flux stabilizes the water column and intermittent convection is suppressed. The heat flux increases rapidly, and within one year it stabilizes. The reason for this development is the reduced heat transport to surface, which was mainly supported by convection under restoring boundary conditions. While the two-box model does not allow horizontal advective and diffusive fluxes into the surface box, the negative heat flux observed in the OGCM can be explained by horizontal advective and diffusive transports at surface.

5.1 Six-box model for the southern ocean

The collapse of the southern deep water formation observed in experiment 30D under mixed boundary conditions will be shown to be a consequence of a delicate interplay of deep convection in the extreme south and shallow intermittent convection in the adjacent

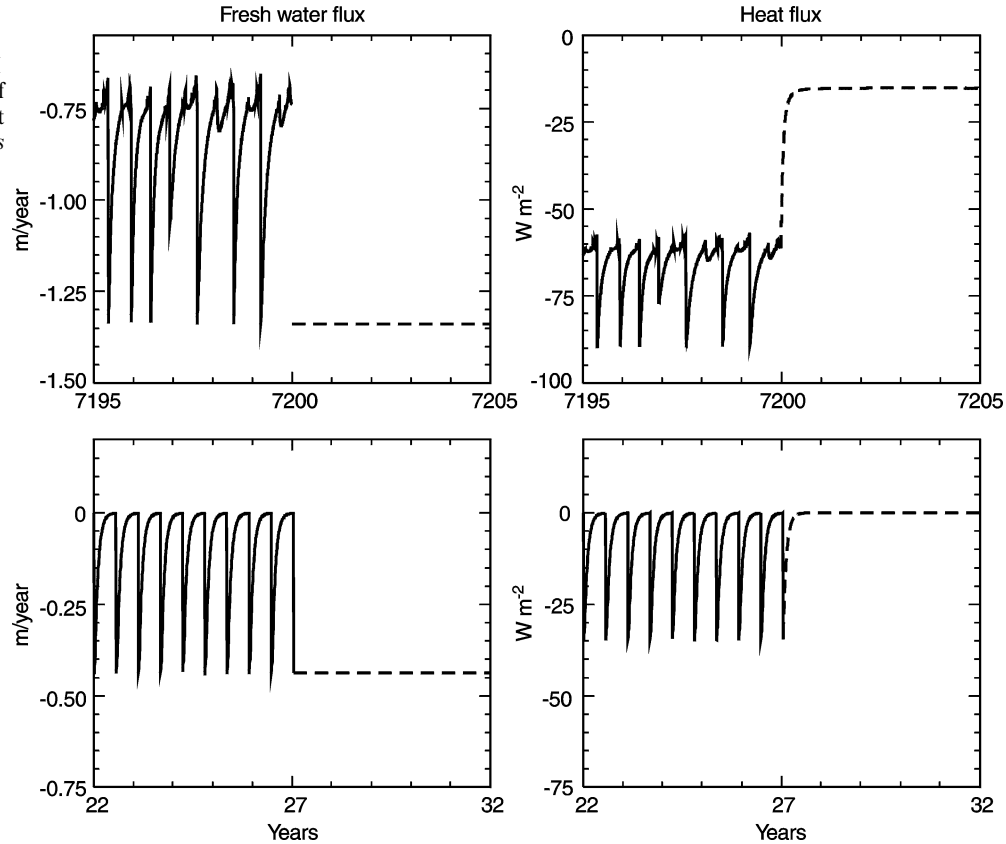

Fig. 14 Comparison of the transition to mixed boundary conditions between the OGCM and the two-box model in case of temperature driven, intermittent convection. The *two upper panels* show the freshwater and heat flux at 72.5 °S/7.5 °W for the OGCM before (*solid lines*) and after switching (*dashed lines*) to mixed boundary conditions. Results of the two-box model are depicted in the *two lower panels*. In the three-dimensional model, as well as in the two-box model, intermittent convection ceases after a switch to mixed boundary conditions

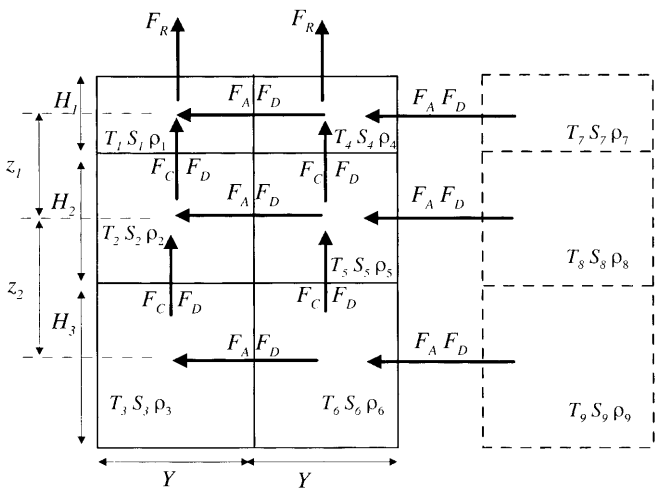

Fig. 15 Six-box model used for analyzing the Southern Ocean. The layer thicknesses are denoted H_i, the mid-depth distances z_i. The temperatures and salinities T_i and S_i are determined by advection A, diffusion D, restoring R and convection C. The restoring temperatures and salinities are denoted T_i^* and S_i^*. The values of T_7, T_8, T_9 and S_7, S_8, S_9 are kept constant so that the dashed boxes behave like infinite reservoirs of heat and salt

water column north of it. Horizontal advection and diffusion of these areas with their surroundings play the essential role. This situation is represented with a simple six-box model shown in Fig. 15.

Table 4 Model parameters for the six-box model

Parameter	Definition	Value
H_1	Thickness	30 m
H_2	Thickness	90 m
H_3	Thickness	4880 m
Y	Meridional extent of grid boxes	$2.77 \cdot 10^5$ m
K_d	Horizontal diffusivity	$2.5 \cdot 10^3$ m^2/s
K_v	Vertical diffusivity	10^{-4} m^2/s
U	Advective velocity	40.5 m/s
$1/\gamma$	Restoring time	30 days

5.2 Model formulation

To compare the six-box model with experiment 30D the thicknesses H_1, H_2 and H_3 correspond to the thicknesses of layers 1, 2–3 and 4–19 of the OGCM (see Table 4). The chosen thicknesses represent the typical depths of convection observed in the OGCM. Shallow convection occurs mostly within layers 1–3. Deep convection typically covers the whole water column down to layer 19.

The meridional extent Y has the same value as in the OGCM. Boxes 1–3 of this arrangement represent the southernmost grid box line (of the "Weddell" or "Ross Sea") in the OGCM, where continuous convection takes place over the whole water column.

Boxes 4–6 represent the northern adjacent grid box with intermittent convection in the upper layers. Temperatures and salinities are kept constant in the boxes 7–9 so that they behave like infinite reservoirs of heat and salt.

The model follows closely the two-box model described before but vertical diffusion with coefficient K_v is added. The model equations (only shown for temperature) read:

$$\frac{dT_1}{dt} = \gamma(T_1^* - T_1) + U\frac{(T_4 - T_1)}{Y}\frac{|\rho_4 - \rho_1|}{\rho_0} + K_d\frac{(T_4 - T_1)}{Y^2} - K_v\frac{(T_1 - T_2)}{z_1 H_1} \quad (7)$$

$$\frac{dT_2}{dt} = U\frac{(T_5 - T_2)}{Y}\frac{|\rho_5 - \rho_2|}{\rho_0} + K_d\frac{(T_5 - T_2)}{Y^2} + K_v\left[\frac{(T_1 - T_2)}{z_1 H_2} - \frac{(T_2 - T_3)}{z_2 H_2}\right] \quad (8)$$

$$\frac{dT_3}{dt} = U\frac{(T_6 - T_3)}{Y}\frac{|\rho_6 - \rho_3|}{\rho_0} + K_d\frac{(T_6 - T_3)}{Y^2} + K_v\frac{(T_2 - T_3)}{z_2 H_3} \quad (9)$$

$$\frac{dT_4}{dt} = \gamma(T_4^* - T_4) + U\left[\frac{(T_7 - T_4)}{Y}\frac{|\rho_7 - \rho_4|}{\rho_0} - \frac{(T_4 - T_1)}{Y}\frac{|\rho_4 - \rho_1|}{\rho_0}\right] + K_d\frac{(T_7 - 2T_4 + T_1)}{Y^2} - K_v\frac{(T_4 - T_5)}{z_1 H_1} \quad (10)$$

$$\frac{dT_5}{dt} = U\left[\frac{(T_8 - T_5)}{Y}\frac{|\rho_8 - \rho_5|}{\rho_0} - \frac{(T_5 - T_2)|\rho_5 - \rho_2|}{Y}\frac{}{\rho_0}\right] + K_d\frac{(T_8 - 2T_5 + T_2)}{Y^2} + K_v\left[\frac{(T_4 - T_5)}{z_1 H_2} - \frac{T_5 - T_6}{z_2 H_2}\right], \quad (11)$$

$$\frac{dT_6}{dt} = U\left[\frac{(T_9 - T_6)}{Y}\frac{|\rho_9 - \rho_6|}{\rho_0} - \frac{(T_6 - T_3)}{Y}\frac{|\rho_6 - \rho_3|}{\rho_0}\right] + K_d\frac{(T_9 - 2T_6 + T_3)}{Y^2} + K_v\frac{T_5 - T_6}{z_2 H_3}. \quad (12)$$

The model parameters are given in Table 4. The values for K_d, K_v and γ were taken according to the OGCM, while the advection coefficient U was chosen in order to achieve an advective transport between boxes 6 and 9 comparable to the meridional overturning simulated in the "Weddell" or "Ross Sea" of the OGCM. As in the two-box model static instabilities are removed by taking the weighted averages and the equations are solved with the explicit Euler–forward scheme.

The restoring values T_1^*, T_4^* and S_1^*, S_4^*, respectively the reservoir values T_7–T_9 and S_7–S_9 were chosen in order to find a spinup state under restoring boundary conditions with continuous convection in boxes 1–3 and intermittent surface convection between boxes 4 and 5. As in the OGCM, convection is temperature–driven in both areas.

At the end of the spinup, temporal variations of the restoring freshwater flux of box 4 reach amplitudes of about 0.75 cm/y, which are of the same order of magnitude of those observed in the OGCM (see Fig. 14). The values of E–P of box 4 are in good agreement with the zonal means depicted in Fig. 11 in box 4, but for box 1 they are lower.

5.3 Comparison with OGCM

Starting from the state of the six-box model after spinup we switched to mixed boundary conditions by using minimum freshwater fluxes as in the OGCM. In Fig. 16 the meridional overturning (see also Fig. 12b), the temperatures and salinities in the Weddell Sea are compared with results of the six-box model. The meridional overturning is compared with the advective transport between the boxes 6 and 9. For temperatures and salinities we took averages of the layers 1, 2–3 and 4–19, at 75 °S and 72.5 °S in the Weddell Sea in order to allow a comparison with the results of the six-box model. The development after transition to mixed boundary conditions is divided into two phases. In the OGCM temporal variations of temperature and salinity related to the intermittent convection observed in the spinup state at 72.5 °S (solid lines) cease at the beginning of phase 1. At this latitude a clear cooling and freshening of the surface occur, while layers 2–3 are slightly warmed. In the initially homogeneous water column at 75 °S small vertical gradients begin to develop between layers 1–3 and 4–19. During this phase changes of meridional overturning remain small. Phase 2 starts about 13 years after the transition to mixed boundary conditions, when strong cooling and freshening occur at 75 °S in layers 1 and 2–3. In the deep layers 4–19 a slight warming and increase of salinity can be observed. Another 2–3 years later the meridional overturning decreases rapidly, and after a further 7 years its value is less than 1 Sv. In both latitudes a clear vertical stratification develops, with low temperatures and salinities at surface and warmer saltier water at depth.

Though the 6-box model is only a rough approximation to the Southern Ocean, it captures quite well the main features observed from the OGCM in this area. In analogy to the OGCM, convection stops between boxes 4 and 5 at the beginning of phase 1 but remains continuous in boxes 1–3. The negative surface freshwater flux in box 4 is no longer compensated by

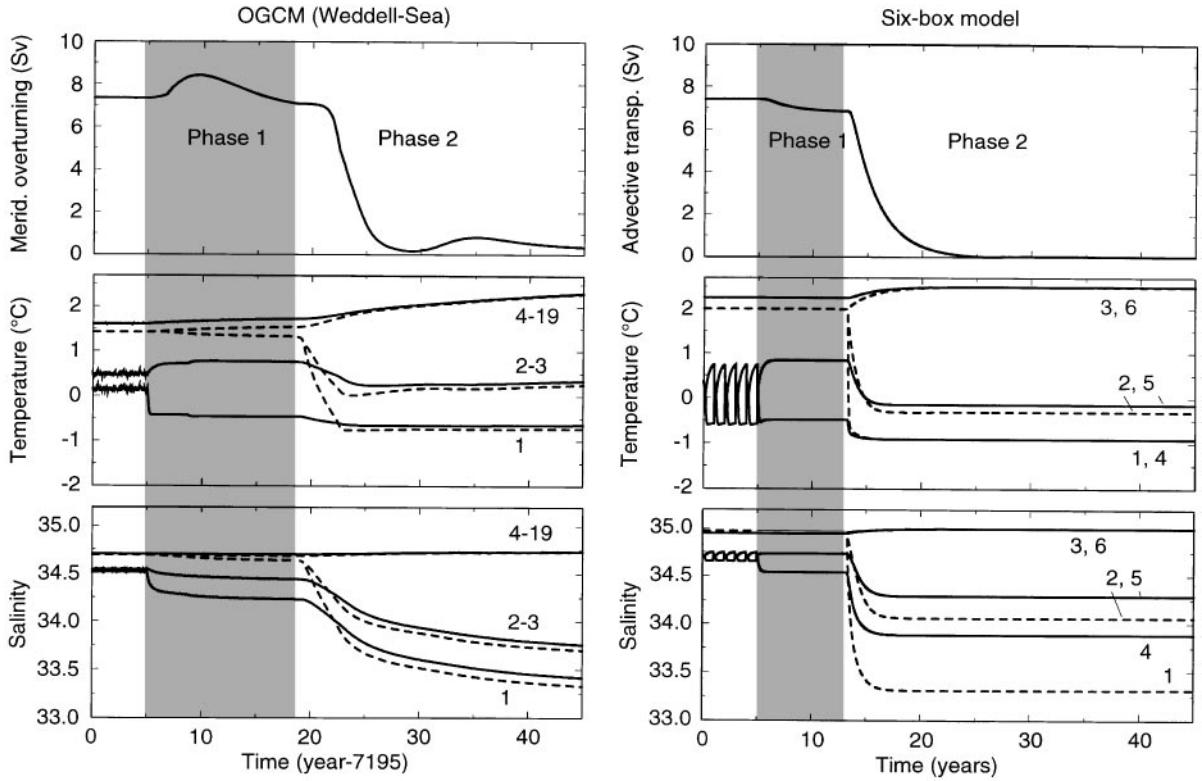

Fig. 16 Comparison of the evolution of overturning, temperature and salinity in the three-dimensional model (Weddell Sea, *left*) and in the six-box model (*right*). Shown is meridional overturning (*upper panel*), temperature (*middle*) and salinity (*lower panel*). For the OGCM temperature and salinity represent zonal means at 75 °S (*dashed lines*) and 72.5 °S (*solid lines*). For the six-box model boxes 1, 2, 3 are drawn with *dashed lines* and boxes 4, 5, 6 with *solid lines*. The *numbers* represent the layers (*italics*) or the box numbers, respectively. The switch to mixed boundary conditions occurs at $t = 5$ y

convection and must be completely balanced by advective and diffusive salt transports. Salinity fluxes for box 4 read (Fig. 15):

$$\bar{F}_R + \bar{F}_{A1} + \bar{F}_{D1} + \bar{F}_C = 0\,, \quad \text{restoring,} \tag{13}$$

$$F_{Rmin} + \bar{F}_{A2} + \bar{F}_{D2} = 0\,, \quad \text{mixed b. c.,} \tag{14}$$

$$\bar{F}_C > 0\,, \quad F_{Rmin} < \bar{F}_R\,. \tag{15}$$

Where $\bar{F}_R$, $\bar{F}_A$, $\bar{F}_D$ and $\bar{F}_C$ are the restoring, advective, diffusive and convective salt fluxes, respectively. Overbars denote time average to average intermittency. Subscript 1 denotes fluxes under restoring boundary conditions, subscript 2 those for mixed boundary conditions. Positive fluxes transport salt into box 4. F_{Rmin} is the minimum of the freshwater flux used under mixed boundary conditions. From Eqs. (13) and (14) it follows that $\bar{F}_{A2} + \bar{F}_{D2} > \bar{F}_{A1} + \bar{F}_{D1}$. Due to the fixed reservoirs (7–9) the increased advective and diffusive transports can only be maintained with a reduced salinity in box 4. Convection between the boxes 1–3 is still continuous during phase 1, so that temperature and salinities remain homogeneous there. The increased advective and diffusive exchange between boxes 1 and 4 tend to stabilize boxes 1–3 with a marginal lowering of the salinity. At the end of phase 1, convection stops in boxes 1–3. During phase 2 the salinities of surface boxes 1 and 4 decrease due to the reduced vertical exchange with the deeper water. A similar behaviour can be observed for surface temperatures, which are rapidly driven towards their restoring values after the breakdown of convection. However, the surface cooling cannot compensate the strong freshening, so the water columns remain stable, with strong vertical stratifications for salinity and temperature. Because of the reduced horizontal gradients of temperature and salinity the advective transport at depth vanishes within 10 yr.

The beginning of phase 2 is marked in the six-box model by an instantaneous breakdown convection with accompanying exponential decrease of the deep advective transport. The OGCM exhibits a lag before meridional overturning ceases. This can be explained by the differences in the driving mechanisms of the meridional overturning in the OGCM and the advective transport in the six-box model. While east–west pressure gradients give rise to meridional overturning in the OGCM, the advective transport in the six-box model is determined by north–south gradients of density, which change exactly at the same time as salinity and temperature do.

6 Conclusions

Based on OGCM circulations achieved under restoring times of 30 days and 150 days we analyzed the processes which lead to intermittent convection and to the sensitivity of deep water formation if mixed boundary conditions are used. Although three different scenarios are conceivable for destabilizing the water column, instability is caused by temperature ($\partial T/\partial z < 0$) in most convective areas of our OGCM experiments. This is also the case in the Southern Ocean where the ocean–atmosphere fluxes show oscillations with a time scale on the order of 100–200 days. Such variations are due to intermittent convection and can be observed even if the OGCM is spun up for more than 7000 yr.

In order to reveal more of the mechanisms responsible for intermittency, we used a simple two-box model for the simulation of convection. We found that intermittency only occurs if the instability of the water column is caused by temperature ($\partial T/\partial z < 0$, $\partial S/\partial z \leqslant 0$) or by salinity ($\partial T/\partial z \geqslant 0$, $\partial S/\partial z > 0$). Although salinity driven intermittent convection was not observed in our OGCM experiments, it is likely to occur in studies of areas where strong evaporation leads to convection (e.g. the Mediterranean Sea, Schott et al. 1988).

As indicated by Pierce et al. (1995), an essential prerequisite for intermittent convection is the non-linearity of the equation-of-state that allows a mixture with higher density than the original water masses. Moreover, intermittency is influenced by the volumes of the water masses mixed during convection, and by the ratio of the heat and freshwater fluxes at surface versus the fluxes at depth. Stable phases between convective events are favored if surface fluxes are stronger than the fluxes at depth. The amplitudes of temporal variations of the ocean-atmosphere fluxes decrease if the restoring time is increased. Depending on the ratios of the water volumes to be mixed during convection and the ratio between diffusive/advective fluxes and the restoring fluxes intermittent convection can occur even for very long restoring times.

Depending on the method employed for calculating the freshwater fluxes used for mixed boundary conditions, the fixed freshwater fluxes lay between the minimum and maximum values which occurred under restoring boundary conditions. This led to different circulations after the switch to mixed boundary conditions. Rapid changes of the convective activity and of the deep water formation occur, similar to the findings of Lenderink and Haarsma (1994).

A detailed analysis of a spontaneous breakdown of deep water formation in the Southern Hemisphere is illustrated with a comparison between a simple six-box model and the OGCM. This shows that the decrease of sea surface salinity can be explained by the interruption of convection in areas where intermittency was observed. The absence of convective fluxes must then be balanced by increased advective and diffusive transports of salt and heat between this area and its surroundings. This stabilizes the adjacent water column with continuous deep convection and leads to the collapse of deep water formation in the south.

In our box-models as well as in the OGCM, intermittency of temperature–driven convection ceases if the ocean–atmosphere fluxes are switched to mixed boundary conditions, i.e. intermittent convection is either stopped (stable state) or it becomes continuous (locally, statically unstable case). Tendencies of the circulation, which were suppressed under restoring boundary conditions can evolve freely. In our OGCM experiments the first consequences are local anomalies of sea surface temperatures and salinities. If these anomalies are adjacent to deep water formation areas, they can lead to major changes of the global ocean circulation. This makes clear that the occurrence of intermittent convection and its behaviour under different boundary conditions are relevant factors for the understanding of the evolution the ocean circulation after the coupling to more realistic ocean-atmosphere fluxes.

Acknowledgements Many thanks are due to GFDL for making the code available and to members of Climate and Environmental Physics in Bern for creating a stimulating working environment. Comments of three reviewers have improved this paper. This work was part of the European project "North-South Climatic Connection and Carbon Cycle over the last 250 ky" and was also supported by the Swiss National Science Foundation.

References

Bryan F (1986) High-latitude salinity effects and interhemispheric thermohaline circulations. Nature 323 : 301–304

Bryan K (1969) A numerical method for the study of the circulation of the world ocean. J Comput Phys 4 : 347–376

Cai W (1996) The stability of the NADWF under mixed boundary conditions with an improved diagnosed fresh water flux field. J Phys Oceanogr 26 : 1081–1087

Carmack EC (1986) Circulation and mixing in ice-covered waters. In: Untersteiner (ed) The geophysics of sea ice. Vol B 146 of NATO ASI, Plenum Press, New York, pp 641–712

Duplessy J-C, Shackleton N (1985) Response of global deep water to Earth's climate change 135 000–107 000 years ago. Nature 316 : 500–507

Duplessy J-C, Shackleton NJ, Fairbanks RG, Labeyrie L, Oppo D, Kallel N (1988) Deepwater source variations during the last climate cycle and their impact on the global deepwater circulation. Paleoceanography 3 : 343–360

England M (1993) Representing the global–scale water masses in ocean general circulation models. J Phys Oceanogr 23 : 1523–1552

Hughes TMC, Weaver AJ (1994) Multiple equilibria of an asymmetric two-basin ocean model. J Phys Oceanogr 24 : 619–637

Karpuz N, Jansen E (1992) A high-resolution diatom record of the last deglaciation from the SE Norwegian Sea: documentation of rapid climatic changes. Paleoceanography 7 : 499–520

Keigwin LD, Lehman SJ (1994) Deep circulation change linked to Heinrich event 1 and Younger Dryas in a middepth North Atlantic core. Paleoceanography 9 : 185–194

Killworth PD (1983) Deep convection in the world ocean. Rev Geophys Space Phys 21 : 1–26
Klinger BA, Marotzke J (1999) Behaviour of double hemisphere thermohaline flows in a single basin. J Phys Oceanogr: In press
Lehman SJ, Keigwin LD (1992) Sudden changes in North Atlantic circulation during the last deglaciation. Nature 356 : 757–762
Lenderink G, Haarsma RJ (1994) Variability and multiple equilibria of the thermohaline circulation associated with deep-water formation. J Phys Oceanogr 24 : 1480–1493
Levitus S, Boyer T (1994) NOAA Atlas NESDIS 3: World ocean Atlas 1994. US Departament of Commerce: National Oceanic and Atmospheric Administration, Tech Rep Vol 4 : temperature
Levitus S, Burgett R, Boyer T (1994) NOAA Atlas NESDIS 3: World ocean Atlas 1994. US Departament of Commerce: National Oceanic and Atmospheric Administration, Tech Rep Vol 3 : salinity
Marotzke J (1991) Influence of convective adjustment on the stability of the thermohaline circulation. J Phys Oceanogr 21 : 903–907
Marotzke J, Willebrand J (1991) Multiple equilibria of the global thermohaline circulation. J Phys Oceanogr 21 : 1372–1385
Mikolajewicz U, Maier-Reimer E (1994) Mixed boundary conditions in ocean general circulation models and their influence on the stability of the model's conveyor belt. J Geophys Res 99 : 22 633–22 644
Pacanowski RC (1995) MOM 2 documention user's guide and reference manual. GFDL, Tech Rep 232 pp
Pierce DW, Barnett TP, Mikolajewicz U (1995) Competing roles of heat and freshwater flux in forcing thermohaline oscillations. J Phys Oceanogr 25 : 2046–2064
Rahmstorf S (1994) Rapid climate transitions in a coupled ocean-atmosphere model. Nature 372 : 82–85
Rahmstorf S (1995) Bifurcations of the Atlantic thermohaline circulation in response to changes in the hydrological cycle. Nature 378 : 145–149
Rahmstorf S, Willebrand J (1995) The role of temperature feedback in stabilizing the thermohaline circulation. J Phys Oceanogr 25 : 787–805
Sarnthein M, Jansen E, Weinelt M, Arnold M, Duplessy J-C, Erlenkeuser H, Flatøy A, Johannessen G, Johannessen T, Jung S, Koc N, Labeyrie L, Maslin M, Pflaumann U, Schulz H (1995) Variations in Atlantic surface ocean paleoceanography, 50°–80 °N: a time-slice record of the last 30 000 years Paleoceanography 10 : 1063–1094
Sarnthein M, Winn K, Jung SJA, Duplessy J.-C, Labeyrie L, Erlenkeuser H, Ganssen G (1994) Changes in east Atlantic deepwater circulation over the last 30 000 years: eight time slice reconstructions. Paleoceanography 9 : 209–267
Schott F, Leaman KD, Zika RG (1988) Deep mixing in the Gulf of Lions, revisited J Geophys Res Letter 15 (8) : 800–803
Stocker TF, Wright DG (1991) Rapid transitions of the ocean's deep circulation induced by changes in surface water fluxes. Nature: 351 : 729–732
Stommel H (1961) Thermohaline convection with two stable regimes of flow. Tellus 13 : 224–241
Street-Perrot F, Perrot R (1990) Abrupt climate fluctuations in the tropics. The influence of Atlantic circulation. Nature 343 : 607–611
Tziperman E, Toggweiler J, Feliks Y, Bryan K (1994) Instability of the thermohaline circulation with respect to mixed boundary conditions: is it really a problem for realistic models? J Phys Oceanogr 24 : 217–232.
UNESCO (1981). Tenth report of the joint panel on oceanographic tables and standards. UNESCO Technical Papers in Marine Sci. No 36. UNESCO, Paris
Weaver AJ, Sarachik ES (1990) On the importance of vertical resolution in certain ocean general circulation models. J Phys Oceanogr 20 : 600–609
Welander P (1982) A simple heat salt oscillator Dyn, Atmos Ocean 1 : 233–242
Whitworth T, Peterson R (1985) Volume transport of the Antarctic Circumpolar Current from bottom pressure measurements. J Phys Oceanogr 15 : 810–816
Wright DG, Stocker TF (1993) Younger Dryas experiments, In: Peltier W (ed) Ice in the climate system. Vol 1 12 of ATO ASI, Springer Verlag, Berlin Heidelberg, New York, pp 395–416